UWB-Based Indoor Localization: How to Optimally Design the Operating Setup?

Gianni Cerro, *Member, IEEE*, Luigi Ferrigno, *Senior Member, IEEE*, Marco Laracca, *Member, IEEE*, Gianfranco Miele, *Senior Member, IEEE*, Filippo Milano, *Student Member, IEEE*, and Valentina Pingerna

***Abstract*— Localizing objects in indoor environments with anchor-based systems poses several challenges to be faced. The main one is the design phase. What is the minimum number of anchors to be adopted? What is the optimal placement of the anchors in the operating domain? These are typical issues that need to be solved in this stage. Such issue is generally addressed by several experimental tests, imposing high costs both in the required large amounts of time and in the use of devices. In addition, sometimes the experiments will not warrant to identify the optimal design solution. In this work, a black-box design tool is proposed, able to manage different environments, in terms of domain size, maximum number of available anchors, device metrological features, and target performance. Such an approach, to be effective, needs a preliminary validation versus experimental results to make the future performance predictions reliable and avoid unexpected localization accuracy degradation. For this reason, the presented work adopts a side-by-side development, by evaluating results' compatibility, in static and dynamic contexts, before addressing further and more complex analyses relying on the design tool only. Such a comparison proves the goodness of the developed design tool, and the outcomes allow an accurate localization system design by finding anchors' placement solutions with the minimum computational burden.**

***Index Terms*— Design tools, indoor localization, optimization, positioning algorithm, ultrawideband (UWB) technology.**

I. Introduction

DEVICES based on the ultrawideband (UWB) technology are often adopted to execute localization in all those applications in which the objects' actions [1] and people's services [2] are tailored to the position they assume in a referenced indoor environment. Examples can be found in those applications where an action is required whenever an object reaches a predetermined indoor position as it happens in modern robot vacuum cleaner, automatic guided vehicles in smart warehouse, autonomous vehicles that perform indoor parking, on-demand augmented reality [3], activation of game experiences [4], or the modern assisted living that provide help to elders or injured people [5]. Localization techniques, methods, and optimization in indoor spaces are widely present in the scientific literature and they span so many technologies and algorithms, from genetic techniques [6], to data fusion based on Kalman filter [7], to Wi-Fi exploitation [8] up to the adoption of Bluetooth and inertial data [9]. Among them, an important role is also played by UWB [10]. The UWB-based localization falls in the so-called anchor-based localization where, at first, the distances of an unknown device (commonly named as "tag") from fixed reference points (typically known as "anchors") is estimated, and then, suitable calculations based on trilateration, triangulation, or the solution of optimization problems are performed to find the optimal triaxial coordinates of the tag which fit the estimated distances [11].

Depending on the specific application, when the realization of a localization system is planned, there are different target key performance indicators (KPIs) that a user would desire to achieve: 1) localization accuracy; 2) power budget; and 3) localization time. As for 1), in many applications it is very important that the localization accuracy of the tag is lower than a defined threshold since worsening in this parameter could invalidate the target application. As far as 2) point is concerned, the power consumption spent from the tag and anchors for each localization is a key parameter especially in those application in which they are battery-operated. This is even more true if we consider that typically, the localization is not the main task that the tag has to perform but it is a complementary service of a wider application. Therefore, localization must not consume all the energy capability of the tag. Finally, as for 3) the time required for each localization is a key parameter that defines a constraint for the speed of mobile devices.

Theoretically, the anchor-based localization is very simple. Once the anchors have been distributed in the localization domain, the measurement of the distance among the tag and the anchors has to be estimated solving a minimization problem. Nevertheless, especially in the design of indoor experimental setups, there are numerous variables that can dramatically invalidate the performance of the system for all the three KPIs considered above.

In detail, fixing the KPIs that have to be reached (i.e., accuracy, power budget, and localization time), the developer

Manuscript received 4 April 2022; revised 5 July 2022; accepted 13 July 2022. Date of publication 29 July 2022; date of current version 9 August 2022. This work was supported in part by the Italian Ministry of Economic Development (MISE) through the "ROBILAUT" Project within the Fondo per la Crescita Sostenibile—Sportello "Fabbrica intelligente" PON I&C 2014-2020 under Grant F/190126/01-02-03/X44. The Associate Editor coordinating the review process was Dr. Sara Sulis. *(Corresponding author: Filippo Milano.)*

Gianni Cerro is with the Department of Medicine and Health Sciences "Vincenzo Tiberio," University of Molise, 86100 Campobasso, Italy (e-mail: gianni.cerro@unimol.it).

Luigi Ferrigno, Gianfranco Miele, Filippo Milano, and Valentina Pingerna are with the Department of Electrical and Information Engineering, University of Cassino and Southern Lazio, 03043 Cassino, Italy (e-mail: ferrigno@unicas.it; g.miele@unicas.it; filippo.milano@unicas.it; valentina.pingerna@unicas.it).

Marco Laracca is with the Department of Astronautics, Electrical and Energy Engineering, Sapienza University of Rome, 00185 Rome, Italy (e-mail: marco.laracca@uniroma1.it).

Digital Object Identifier 10.1109/TIM.2022.3194924

of localization services based on UWB technology has to face some important issues as: 1) the minimum number of anchors; 2) the optimal placement of the anchors; and 3) the minimum number of repeated measurements that the tag has to execute for each localization. Unfortunately, all these parameters cannot be chosen for a generic application and once and for all because they are strongly dependent on the real characteristics of the localization domain in which the application is developed, the uncertainties of the considered anchors and tag in the ranging phase, the measurement time, the power consumption of the devices, the communication protocol (i.e., number, rate, and payload of messages), etc. This makes the development of the localization application a complicated task in which many experiments have to be done to optimize the aspects of interest. This leads on one hand to an increase in development times and costs and on the other hand does not guarantee to have found the optimal solution to the problem.

In this operating scenario, the availability of a design tool capable of optimizing the choice of the parameters from 1) to 3) according to the achievement of one or more of the considered KPIs could dramatically minimize the time and costs for the design of localization system for specific applications.

For these reasons, starting from what is stated in [12] and stemming from their past experience in localization systems [13], [14], the authors, in this article, extent their research proposing a first step for the realization of a fully flexible design tool, able to optimize 1)–3) input parameters. In detail, at the moment, the developed design tool returns the best configuration in terms of minimum number of anchors and their optimal arrangement to allow the achievement of the target localization accuracy or better configuration if none of the considered is able to achieve the goal. An experimental validation stage is proposed in this article comparing the obtained results with those experienced using the DecaWave [15] UWB kit in both static and dynamic conditions. In addition, together with Decawave, this article also proposes some tests considering the performance of other two UWB devices, namely, the BeSpoon [16] and the Ubisense [17].

In detail, the main contributions of this article are as follows.

1) The definition of a simulation-to-experimental transfer tool able to accurately predict localization performance levels whenever knowledge about the involved uncertainty models can be inferred and the device metrological features are known.
2) The formalization of an optimization model able to deliver suitable configurations to the implementers by balancing performance and energy constraints.
3) A methodology to compute the uncertainty model to be associated with the joint combination device environment instead of using only datasheet-derived contributions and without adopting complex radio-propagation models. In the UWB case, it gives out very promising results. The generalization needs further investigation.

This article is organized as follows. Section II provides a brief discussion of the state-of-the-art. Section III presents the developed design tool. The experimental validation with a real UWB kit is presented in Section IV, where UWB attractive features are also described. The results from the design tool are reported and discussed in Section V. Conclusions and future developments are finally described in Section VI.

II. State-of-the-Art in Simulation Techniques for Indoor Localization

In the scientific literature regarding the development of localization design tools, some efforts have already been carried out. In particular, to the best of our knowledge, most scientific contributions to the field are related to the analysis of the signal propagation in a defined indoor or outdoor environment considering the line of sight (LoS) and non LoS (NLoS) conditions, the issues related to radio-propagation, and the outputs related to those effects. They do not provide the user with optimal design parameters, in terms of anchors arrangement, given a specific localization device and an application environment. As an example, Gigl *et al.* [18] perform simulation on UWB technology by analyzing processing type (positioning and tracking methods), visibility conditions (LoS versus NLoS), receiver modeling, and signal processing techniques to get distances. The output of this article is the error cumulative distribution functions (cdfs) due to the different aspect they consider in the simulations. The work does not provide design criteria or optimal receiver placement to help designers in the experimental setup implementation. Another contribution is provided by Amiot *et al.* [19], where the authors simulate the usage of different radio access technologies and focus their attention on radio-propagation issues in such environment where possible obstacles could be present, as walls. The output is a map of the signal received power levels in different points of the localization domain. The authors do not provide any indication about the localization performance and do not consider any metrological aspects on the adopted devices. Jankowski and Nikodem [20] develop a simulator for indoor localization adopting the time difference of arrival (TDoA) or time of flight (ToF) measurements. They use two different static anchor configurations and adopt three processing techniques for positioning purposes and compare the obtained results, also analyzing the effect of clock drifts on the localization error. Their output is the estimation of the localization error, also defining possible localization black zones where their simulator does not provide any result, due to issues related to configuration and processing. This article does not investigate the effect of the number of adopted anchors and their variable arrangement in the localization domain. Finally, an interesting article is presented by Pérez-Rubio *et al.* [21]. It faces the localization based on ultrasonic signals. The authors develop a simulator, which allows to design several aspects related to transmission/reception of signals among ultrasonic devices and an online demonstrator, which can be used to validate choices derived from the simulation. To our understanding, still the simulator does not allow changing the number of available devices considered in the demonstrator and their arrangement, and it is not possible to perform an optimization process to get the best configuration.

III. Proposed Design Tool

In this section, details about the proposed design tool are given. It can be used as a suitable support to design

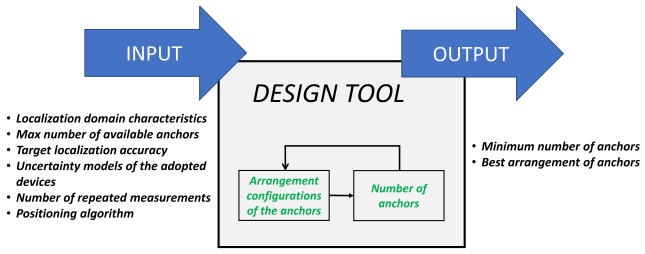

Fig. 1. Black-box schematic of the design tool with input–output parameters.

an anchor-based localization system that adopts UWB technology. The design tool is able to manage different input parameters (localization domain features, uncertainty model of the adopted devices, etc.) and different constraints (energy consumption, maximum number of available anchors, etc.) and performs simulations with the aim of determining the configuration and the optimal number of anchors to respect performance and cost constraints.

In particular, the tool works by calculating Euclidean distances (calling them as *ideal ranges*) between the anchors and tag (whose positions are given as input) and perturbing them (namely, *perturbed ranges*) by means of known uncertainty models, depending on the adopted devices and the considered test environment. On the perturbed ranges, tag positions are computed and the localization error is calculated. To exploit tool capability, different cases and application scenarios have been considered. In particular, two examples of different anchors' arrangement ways and three different devices' metrological features have been analyzed.

A. Simulation Parameters

The proposed design tool was developed in the MATLAB environment. Fig. 1 shows a black-box schematic of the design tool with a highlight of the input–output parameters as described below.

1) The localization domain characteristics are connected to the size and shape of the domain in which the designer has to perform the localization system design. Inside this domain, as better described below, it is possible to chose the subdomains in which the anchors can be placed and tag localization has to be performed. Another important feature is that the simulator allows considering the uncertainty model of the localization domain. In particular, since the environment plays a crucial role in terms of signal propagation and obstacles that are placed in the proximity of the localization domain, its effect will affect the overall performance. The possibility to take into account these effects will provide more reliable simulation results. These effects can be estimated using *a priori* information derived from electromagnetic modeling of the environment features or by means of an experimental campaign on the given location. In this second case, the uncertainty model of the localization domain can be considered in the repeatability contribution of the uncertainty model of the adopted device (as better described in Section III-B).
2) The maximum number of available anchors can be defined starting from the size of the domain and the maximum desired overall power budget (connected to the energy consumption of each anchor).
3) The target localization accuracy represents the desired accuracy performance of the designed localization system (later named as "error threshold").
4) The uncertainty model of the adopted UWB devices. In particular, this model takes into account the accuracy and repeatability contributions, as detailed in Section III-B.
5) The number of repeated measurements, made for each anchor–tag ranging phase, is obtained by a compromise between localization accuracy, localization time (that defines the dynamic performance of the localization system), and energy consumption. The value provided as input can be the maximum number of repeated measurements to be made to accomplish for the mentioned constraints or a range of values in which the tool has to perform the optimization.
6) The positioning algorithm to be adopted for the localization task. It can be used as "standard" algorithms, but it can also be customized by the users that can add its own algorithm script.

Inside the design tool, different ways of arranging anchors within the localization domain and variable number of anchors can be implemented. As far as the arrangement configuration of the anchors, the areas where the anchors can be positioned are defined considering the input constraints. These can be identified as subdomains, inside the localization domain, considering the available planes and inside that the available areas in which the anchors can be placed (depending on the constraints due to the application or on the specific features of the localization domain such as engaged areas of the planes). In particular, in each defined area a regular grid of points in which the anchors can be positioned is defined. In this way, the design tool can optimize the performance of the localization system to be designed considering the minimum number and the best arrangement of the anchors, which can be picked up as outputs.

The design tool allows the optimization of all the variable parameters (highlighted in green in Fig. 1) by setting the values (or ranges) of the input parameters.

B. Design Tool Step by Step

Fig. 2 shows the iterative procedure performed by the design tool.

1) *Initialization:* The initial phase (initialization in Fig. 2) is the acquisition of all the input parameters of the design tool (i.e., the parameters described in Section III-A). After the acquisition of the input parameters, the initialization phase is completed by the definition of the tag points' positions on which the design tool evaluates the localization performance as a global localization domain parameter. Tag points' definition is performed by means of a domain discretization according to a uniform points' grid, useful to evaluate the localization

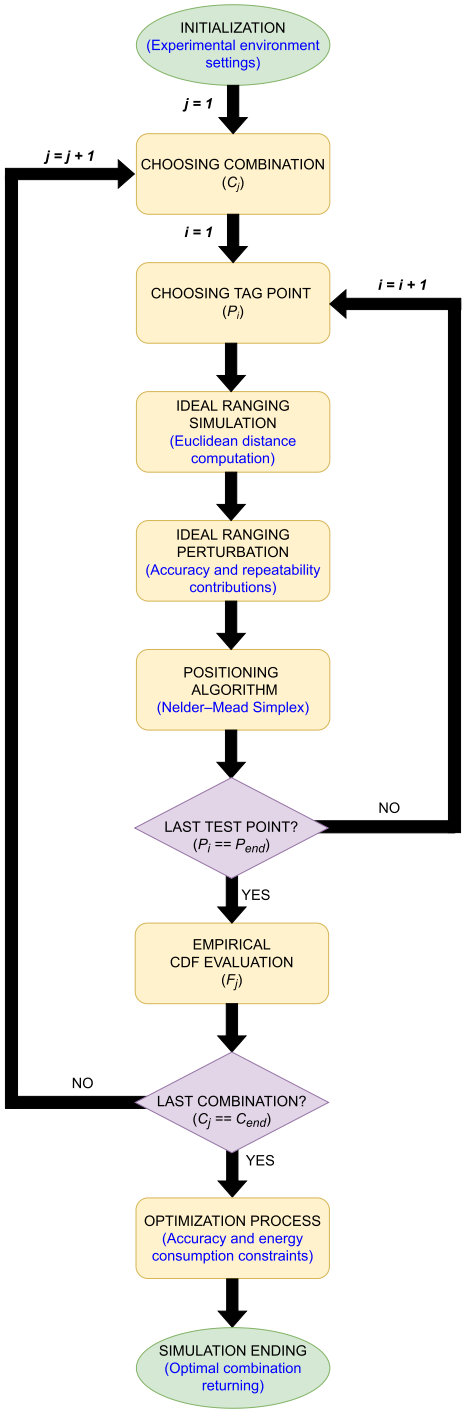

Fig. 2. Design tool's performed operations in logical order.

accuracy in a balanced way. Similar to the management of the arrangement configuration of the anchors, it a localization subdomain can be defined in which the tags can be placed according to the constraints of the areas in which the localization task has to be performed. The set of all tag points represents the discretized domain.

2) *Choosing Combination:* Among the variable parameters (highlighted in green in Fig. 1), a specific combination of them is here chosen to perform the simulation. The generic combination of these parameters is identified as C_j within the flowchart.
3) *Choosing Tag Point:* The second step is the choice of one of the tag points in the domain regular grid. The chosen tag point is identified as P_i within the flowchart.
4) *Ideal Ranging Simulation:* Regarding the chosen tag point (P_i), ideal ranges between each anchor and P_i itself are computed. Each ideal range takes into account only the anchors' position and tag coordinates, for which the Euclidean distance is computed.
5) *Ideal Ranging Perturbation:* Considering the device metrological features, the contribution of device accuracy and repeatability, which takes into account also the environment where the localization test is performed, is added to perturb the ideal ranges, allowing to obtain the perturbed ranges. The perturbation phase is performed according to the available information. In detail, it is anyway composed of the addition of an accuracy and repeatability contribution to the ideal range. The estimation of such quantities can be derived from an experimental characterization performed on real environment, and therefore it accurately includes all the effects also due to obstacles and unexpected reflections. It is anyway possible that such characterization is not available or it is performed on a different environment: in such a case, the perturbing parameters will slightly differ from the actual one and performance could be consequently influenced. Whatever be the source of perturbing information, the process is described in Fig. 3). The ideal range (r_{ideal}) is considered as the mean value of a uniform distribution, having the half-width equal to the accuracy (A). The output of the uniform random variable (r_{bias}) is then used as the mean value of a Gaussian random variable, whose variance (σ^2) is the square of the considered device's repeatability. The outcome of the Gaussian random variable is the perturbed range (r_{pert}) for each couple anchor–tag. In the specific case of UWB localization, the effects of different environments are minimized due to the UWB propagation model [22].
6) *Positioning Algorithm:* Such perturbed ranges are then used in the positioning algorithm, where the tag position P_i is estimated. The positioning algorithm can be chosen and/or customized by the user. As far as the analysis presented in this article, the Nelder–Mead Simplex method is used. Details on the structure of the positioning algorithm are given in our previous article [13], where the algorithm is applied to magnetic measurements: in this case, and the only modification is the adoption of ranges in the objective function instead of magnetic field measurements.

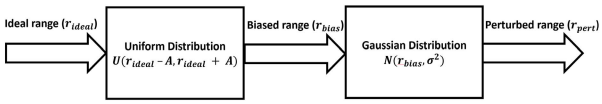

Fig. 3. Block diagram for the perturbation of ideal ranges.

7) *Last Test Point?:* This checkpoint verifies whether all the tag positions have been tested: in the positive case, the next step is performed; otherwise, it goes back to choosing the tag point step.
8) *Empirical CDF Evaluation:* After all the tag points have been analyzed, it is possible to evaluate the localization errors and their empirical cdf (later named F_j). The localization error ($\|\varepsilon\|$), according to (1), was defined as the Euclidean distance between the true ($\vartheta = [x, y, z]$) and estimated position ($\tilde{\vartheta} = [\tilde{x}, \tilde{y}, \tilde{z}]$) of the tag, respectively. The difference between the single coordinates on the axes x, y, and z of the true position and the estimated position is represented by ε_x, ε_y, and ε_z, respectively,

$$\|\varepsilon\| = \sqrt{\varepsilon_x^2 + \varepsilon_y^2 + \varepsilon_z^2} \tag{1}$$

$$\varepsilon_i = \vartheta_i - \tilde{\vartheta}_i, \quad i \in \{x, y, z\}. \tag{2}$$

In particular, according to (2), ϑ_i is the true coordinate of the tag and $\tilde{\vartheta}_i$ is the estimated coordinate of the tag. Subsequently, when experimental tests are carried out, $\tilde{\vartheta}$ represents the estimated tag position through the experimental setup; instead, when simulated tests are performed, $\tilde{\vartheta}$ represents the estimated tag position by the design tool. The same distinction applies to the localization error $||\varepsilon||$.
9) *Last Combination?:* This checkpoint verifies whether all the possible combinations in terms of variable parameters have been tested: in the positive case, the next step is performed; otherwise, it goes back to choosing the combination step.
10) *Optimization Process:* Once all the possible combinations (N) of the variable parameters have been tested ($C_j = C_{\text{end}}$), each of these combinations corresponds to F_j. These cdfs represent the input of the optimization process which aims to identify the best combination C_j subjected to predefined constraints. In detail, the optimization process aims to obtain the combination C_j with the lowest number of anchors able to guarantee the achievement of target localization accuracy.
To do this, an objective function directly proportional to the adopted number of anchors for the generic combination (C_j) was defined. In particular, the objective function (E_c) refers to the energy consumption of the system, therefore directly proportional to the adopted number of anchors. The minimization process of E_c is subject to the constraint that the value of the cdf (F_j) at the fixed error threshold (ε_{th}) must be greater than 0.9. In this way, the obtained result $\tilde{j}$ from (3) represents all those combinations that guarantee the constraint on the localization error ($F_j(\varepsilon_{\text{th}}) \geq 0.9$) with the same number of anchors, or in case no combination can guarantee the imposed constraint, $\tilde{j}$ will include all the combinations having the maximum number of anchors, independently of the constraint value

$$\tilde{\mathbf{j}} = \arg \min_{j \in [1,N]} E_c(j) \quad \text{s. t.} \quad F_j(\varepsilon_{\text{th}}) \geq 0.9. \tag{3}$$

Finally, the combination (k^*) that maximizes the value of cdf at the fixed error threshold is chosen (4) from among all the combinations obtained from (3)

$$k^* = \arg \max_{k \in \tilde{\mathbf{j}}} F_k(\varepsilon_{\text{th}}). \tag{4}$$

11) *Simulation Ending:* Combination k^* is returned as optimal by the design tool.

IV. Experimental Validation

A. Ultrawideband Technology

Nowadays, one of the most used localization technologies is the UWB which is based on the transmission of energy pulses of extremely short duration (typically of the order of nanoseconds or picoseconds) and with very wide spectral occupancy. A UWB device generates a radio frequency (RF) signal that occupies a portion of the frequency spectrum that is greater than 20% (up to 110%) of the center carrier frequency or has a bandwidth greater than 500 MHz (up to 7.5 GHz). The high bandwidth gives the antennas the ability to transmit large amounts of data with low power consumption. The presence of these features allows to obtain advantages such as the ability to penetrate through obstacles, high immunity to interference, and multipath effects [22]. The cited features allow an easy adoption in localization systems, since effects of the localization domain structure can be neglected with low impact on localization performance. The use of this methodology allows high-speed data transmission, with the possibility of estimating the position in a very accurate way, even when compared with other existing systems [23]. In general, the main components of such a system are antennas that behave as anchors, one (or more) antennas as target and the necessary software and hardware support. Using, for instance, the TDoA of the RF signals, it is possible to obtain an indication regarding the distance between the anchor and target nodes. Using, then, the information relating to the distances within the positioning algorithms, it is possible to obtain the unknown position of the target. Due to limitations on transmit power, applications using UWB signals are limited to those transmitting short range and high speed or long distance and low speed [24].

B. Adopted Development Kit

The kit used for validation is *TREK1000*, equipped with the DW1000 chip, produced by the DecaWave company [15] that develops semiconductor solutions, software, and modules that enable real-time and ultra-accurate local area microlocation services. The kit is able to evaluate the performance of the DW1000 chip in real-time environment. TREK1000 contains four configurable units as anchor or tag, where the single unit is shown in Fig. 4, compliant with IEEE802.15.4-2011 UWB [25] and with data rates up to 6.8 Mb/s, an ARM Cortex M3 STM32F105 processor and an omnidirectional antenna. The system supports data rates of 110 k/s, 850 kb/s, and 6.8 Mb/s and covers six RFs bands from 3.5 to 6.5 GHz. The evaluation kit allows distance measurements with an accuracy of ± 10 cm using two-way ranging ToF measurements.

C. Validation of the Ranging Perturbation and Positioning Algorithm

To validate the adopted range perturbation model and the positioning algorithm within the design tool, the obtained

Fig. 4. Configurable UWB module in the TREK1000 evaluation kit from Decawave [15].

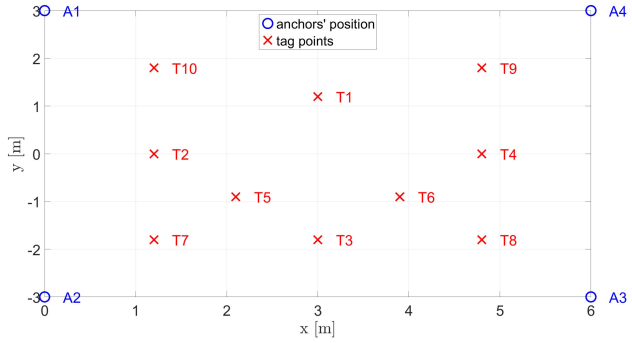

Fig. 5. Positions of anchors and tag points in the experimental setup adopted for the static validation purpose.

TABLE I
COORDINATES OF THE TAG POINTS IN STATIC SCENARIO

Tag points	x [m]	y [m]	z [m]
1	3.0	1.2	1.12
2	1.2	0.0	1.0
3	3.0	-1.8	1.12
4	4.8	0.0	1.12
5	2.1	-0.9	0.48
6	3.9	-0.9	1.12
7	1.2	-1.8	1.0
8	4.8	-1.8	1.0
9	4.8	1.8	1.12
10	1.2	1.8	1.12

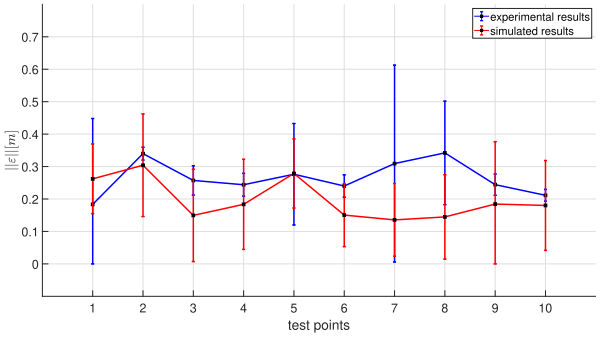

Fig. 6. Obtained localization errors for the experimental data (in blue) and the simulated data (in red) in static environment. The vertical bars represent the standard deviation of the 100 repeated measurements.

results in the experimental measurements were compared with those obtained from the simulated environment, where ideal range perturbation (as explained in Section III-B) has been carried out by means of kit's datasheet (accuracy contribution) and repeatability estimation from [23]. Such validation has been carried out both in static and dynamic contexts.

All the devices, both anchors and tag, need to be powered by a 5-V dc source. The energy can be provided by batteries or USB connections to a personal computer. In both validation contexts, portable batteries (power banks) were used to power the anchors, while the tag was connected to a raspberry pi 4, acting as a data aggregator. The raspberry pi is used to collect all the measured anchor–tag ranges, estimated by the tag itself to obtain its position. The raspberry pi was also powered by a power bank.

1) Localization Tests in a Static Scenario: The indoor experimental setup was assembled considering the anchors and tag positions as shown in Fig. 5. Four anchors (A1–A4) are placed in known coordinates and at the same height ($z = 1.5$ m) from the ground floor. Within the localization domain (that has a size of $6 \times 6 \times 1.5$ m^3), the tag points (T1–T10) were traced along ten positions. The Cartesian coordinates of the tag points are reported in Table I. For each localization point, 100 repeated measurements were performed. The same operating conditions were used in the simulated environment. Therefore, the total number of test cases is ten tag point times 100 repeated measurements per tag point, i.e., 1000 tests. In each test, the localization error was adopted to evaluate the localization performance. Fig. 6 reports the error bar plots for both the simulated and experimental localization processes in a static scenario. For each test point, a vertical bar is reported for both the cases. The bar center is localized in correspondence with the mean localization error value over the 100 repeated measurements, while its half-length corresponds to the computed and expanded standard deviation of the mean. The overlapping of the bars in each test point confirms the measurement compatibility between the simulated and experimental data, thus validating the simulator's capability to predict real localization performance. The addressed confidence level is 99.7% under Gaussian assumption, i.e., the standard deviation of the mean (type A uncertainty) has been expanded by a factor of 3. In detail, it is possible to highlight a performance worsening in terms of repeatability quantified by standard deviations in the experimental results, particularly visible on points 1, 7, and 8. Furthermore, a light increase in the mean error value can be seen, which ranges from 0.20 m in the simulated results to 0.26 m in the experimental case. It is anyway possible to state measurement compatibility between the obtained set of measurements. This confirms the goodness of the adopted methodology.

2) Localization Tests in a Dynamic Scenario: To test the adopted perturbation on dynamic conditions, a similar validation procedure has been carried out in a dynamic scenario larger ($25 \times 50 \times 2$ m^3) than the static case. As shown in Fig. 7, to achieve total coverage throughout the localization domain, eight anchors (A1–A8) were used. The anchors share the same height equal to 2 m. The test was performed by moving the tag with a speed equal to 0.50 m/s along a rectangular path (true path) characterized by four segments

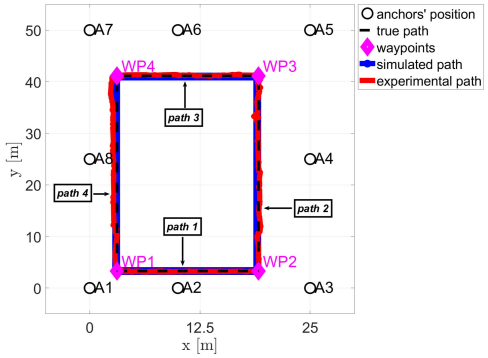

Fig. 7. Positions of anchors and waypoints in the experimental setup adopted for the dynamic validation purpose.

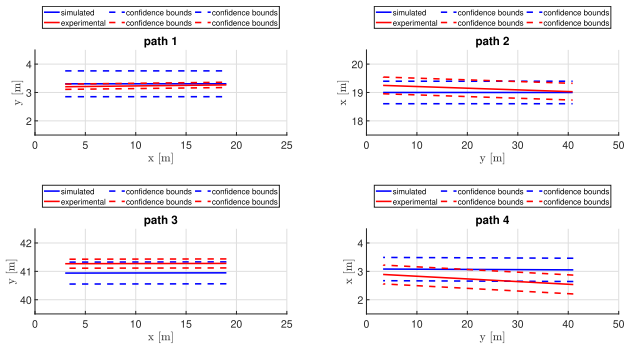

Fig. 8. Path-by-path trajectory compatibility evaluation—dynamic scenario.

path 1–path 4 whose intersections are named as waypoints (WP1–WP4). As regards the experimental test, we adopted a tele-operated vehicle moving the tag and sampling the tag position estimation at 0.1-s rate. In terms of test cases, one localization per tag point has been performed along paths 1–4, while 100 repeated measurements have been carried out in the four waypoints: WP1–WP4. Considering the cited parameters, 320 localizations tests each are computed in case of path 1 and path 3, 754 localizations each for paths 2 and 4, and 400 cumulative tests in WP1–WP4. Considering common points, a total number of 2540 tests have been performed in the dynamic scenario. The validation has been performed on two levels: trajectory compatibility and waypoint localization error comparison. The first one aims to evaluate whether the trajectory followed by the experimental test and the one derived from simulation are compatible. This is achieved by splitting the trajectory analysis into the four defined segments (path 1–path 4) (as reported in Fig. 7), characterized by the constancy of one of the coordinates.

1) *Path 1:* $x \in [3, 19]$ m, $\mathbf{y = 3.3\ m}$.
2) *Path 2:* $\mathbf{x = 19\ m}$, $y \in [3.3, 41]$ m.
3) *Path 3:* $x \in [3, 19]$ m, $\mathbf{y = 41\ m}$.
4) *Path 4:* $\mathbf{x = 3\ m}$, $y \in [3.3, 41]$ m.

For each path, a linear fitting of the followed trajectory has been performed for both the simulated environment and experimental tests. The obtained lines have been bounded by a confidence interval at 95%, obtained from standard deviations as in the static case. The results are provided in Fig. 8. As reported in Fig. 8, a 99.7% compatibility between the experimental tests and simulation is achieved for

TABLE II
COORDINATES OF WAYPOINTS IN DYNAMIC SCENARIO

Waypoints	x [m]	y [m]	z [m]
WP1	3.0	3.3	1.0
WP2	19.0	3.3	1.0
WP3	19.0	41.0	1.0
WP4	3.0	41.0	1.0

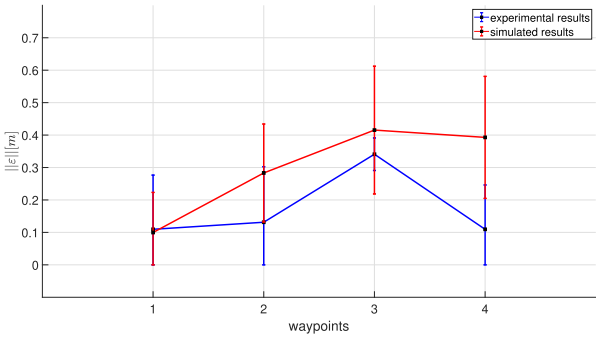

Fig. 9. Obtained positioning errors for the experimental data (in blue) and the simulated data (in red) in dynamic environment.

all the segments. As regards the waypoint localization error comparison, the same procedure than in the static case has been followed. The Cartesian coordinates of the waypoints are shown in Table II. The obtained results in the four waypoints are shown in Fig. 9, both for the experimental setup and for the simulated environment. In terms of mean error values, the experimental results provide 0.17 m against 0.29 m obtained in the simulated environment, while standard deviations are generally comparable in all the considered points. As happened for the validation in the static context, here results are within a 99.7% confidence interval. Compatibility among results is directly evaluated in the waypoints, since these are the only locations where the vehicle has been stopped for a longer time period, to obtain repetitive position estimations and, consequently, possible standard deviation computation. In such points, the measurement compatibility is ensured. A general consideration is necessary here about error quantification and its suitability to application purposes. In the experimental case and, whenever the simulator is correctly designed, also in the simulation environment, the error magnitudes are dependent on several influence factors. Just to cite a few, the environment, the acquisition system, the ranging phase estimation, the positioning technique. Nevertheless, obtained error mean values are fully in-line with the TREK1000 user manual [15], which assumes devices committing a 30-cm error in 2-D/3-D real-time location scenarios. Considering that the algorithm optimization to get minimal localization error for a fixed configuration is out of the scope of this article and the compatibility of the simulated output with the experimental findings is warranted, the obtained errors are also reasonable in terms of what the adopted devices are expected to provide.

V. APPLICATION OF THE DESIGN TOOL ON SOME CASE STUDIES

After carrying out the validation tests, a series of scenarios were simulated to show the usability of the proposed

TABLE III
MAIN PARAMETERS OF THE SIMULATION SCENARIO

Parameter	Value
Domain Size	15x15x3 m^3
Maximum number of anchors	12
Target Localization accuracy	0.1 - 1 m
Uncertainty Model (Gaussian)	Accuracy and Repeatability
Number of repeated measurements	100
Positioning Algorithm	Nelder-Mead Simplex

tool for the design of an anchor-based UWB localization system.

A. Simulation Parameters' Values

As previously described, the design tool accepts various input parameters to provide the best configuration in terms of number and spatial arrangement of the anchors. In principle, all the input parameters can vary in a specific range, defined by the constraints of a specific application field. To highlight the results most closely related to the design aspects of a localization system, some of these parameters have been considered fixed, while other ones as variable. It is important to state that the obtained results, discussed in the following, are related to the input parameters' choice and they are not to be generalized. In other words, stated that the aim of the tool is to find the optimal solution in terms of anchors arrangement and minimum number of anchors that satisfy the chosen input parameters/constrains, the organization of the experimental validation previously described in Section IV-C and the simulations reported below are organized to prove the design tool capabilities. In this framework, for each input parameter to the design tool, details about the considered values are provided below and summarized in Table III.

1) *Localization Domain Characteristics:* The size is equal to $15 \times 15 \times 3$ m^3 according to a parallelepiped shape. This choice is consistent with the typical applications of UWB technology.
2) *Maximum Number of Available Anchors:* It is equal to 12. Furthermore, since it is an unconstrained 3-D localization problem, the minimum number of available anchors is 4.
3) *Target Localization Accuracy:* These values have been identified on the basis of the quality of the localization systems based on the UWB technology. Specifically, they depend of the considered application, and in the analysis reported in this article error thresholds from 0.1 to 1 m were considered.
4) *Uncertainty Model of the Adopted UWB Devices:* To vary the device metrological features, three different UWB kits were considered (Decawave [15], BeSpoon [16], and Ubisense [17]). The accuracy and repeatability values have been extracted from the datasheets of the devices and [23], respectively, as detailed below.
    a) Accuracy contribution indicates, for each range, the deviation between the estimated range and the corresponding ideal one. This quantity has been modeled as a uniform random variable $U([a, b])$ in which the definition interval $[a, b]$ depends on the ideal range (r_{ideal}) and the accuracy value (A) of the device, as reported in the first block of Fig. 3. In particular, consulting the datasheets of devices Decawave, BeSpoon, and Ubisense, the A values are 10, 10, and 15 cm, respectively.
    b) Repeatability contribution is evaluated by means of standard deviation of repeated measurements [23]. To carry out the standard deviations (σ) of ranges measured by the three UWB kits, Ruiz and Granja [23] divided the analysis interval (0–25 m) into five distance–intervals (between anchor and tag) having 5-m size. In this way, for each kit, there are five standard deviations corresponding to the five analyzed distance–intervals. Fig. 10 shows all the standard deviations of the measured ranges during the experimental campaign carried out by Ruiz and Granja [23]. Such values become the homonym parameter of a Gaussian distribution (different kit by kit) having as mean value r_{bias}, i.e., the outcome of the first block of Fig. 3. The final result r_{pert} is adopted as perturbed range in the design tool. The following holds.
5) *Number of Repeated Measurements:* It is fixed at 100 in this experimental campaign, but it could vary and be optimized as well.
6) *Positioning Algorithm:* The Nelder–Mead Simplex algorithm [13] is adopted in this experimental campaign but it can be customized by the user.

To properly analyze the possible outputs of the design tool with respect to the location and the number of anchors, two suitable configuration choices have been made. It is important to state that both the considered environment and the chosen configurations do not constrain the design tool, which can work in any domain, having objective features to be extracted and inputted to the tool itself, and can provide whatever optimal configuration having the least number of anchors, the target localization accuracy, and being respected the energy constraint. As an example of operating conditions, two configurations are reported in this section and detailed below.

1) Configuration 1 allows to increase the number of anchors by progressively occupying all the available planes of the localization domain. Fig. 11 shows the spatial arrangement of the anchors according to configuration 1. It is noted that the first four anchors available (A1–A4) occupy a single plane of the domain ($xz, y = 0$ m); increasing the number of anchors up to 8 also the plane $yz, x = 15$ m will be totally occupied. Finally, increasing the number of anchors up to 12, other two planes ($xz, y = 15$ m and $yz, x = 0$ m) will be totally occupied. In this way, planes, areas within planes, and the corresponding grid points have been defined. This configuration is thought as a possible arrangement way whenever the localization domain boundaries cannot be fully occupied, e.g., in a museum where some sides are occupied by pieces of art.
2) Configuration 2 allows to increase the number of anchors to uniformly fill all the four planes of the localization

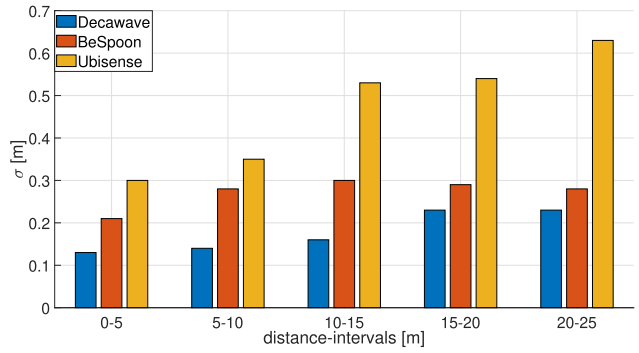

Fig. 10. Experimental standard deviations (σ) of the estimated ranges for the three UWB kits [23] versus the distance–intervals between the anchor and the tag.

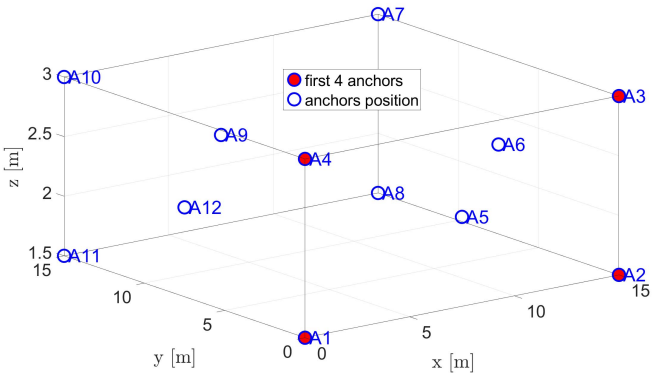

Fig. 11. Schematic of the simulated setup in configuration 1.

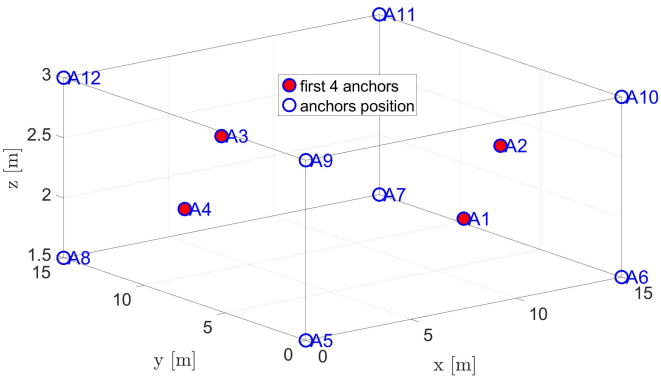

Fig. 12. Schematic of the simulated setup in configuration 2.

domain described in configuration 1. Fig. 12 shows the spatial arrangement of the anchors according to configuration 2. Considering the first four anchors (A1–A4), all the planes of the domain are occupied since the four anchors are arranged in the middle of each plane. Increasing the number of anchors up to 12, all the corners of the localization domain will be progressively occupied. This configuration is thought for cases when only floor and roof cannot be occupied by anchors and the number of anchors per plane should follow symmetry rules.

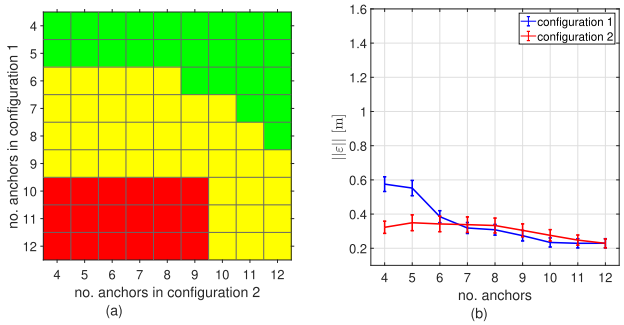

Fig. 13. Performance comparison between configurations 1 and 2. (a) Color map indicating the best configuration versus the number of anchors: green for configuration 2, red for configuration 1, and yellow in case of compatible results. (b) Norm of the localization error versus the number of anchors for both the configurations in the form of error (standard deviation) bar. DecaWave case.

To evaluate the performance of the design tool, the localization domain was discretized into 216 equally distributed tag points. For each tag point, 100 repeated ranging measurements were carried out and the same number of estimated tag positions is obtained. The localization error is then computed on the mean position value for each tag point as ($||\varepsilon||$).

B. Results

Given the desired target localization accuracy, to provide an optimal configuration in terms of number and spatial arrangement of the anchors, several simulations were carried out by varying the input parameters within their own defined ranges described in Section V-A.

Initially, a comparison between the two adopted configurations for the arrangement of the anchors was carried out for each considered UWB kit. Such comparison on chosen configurations has the goal to prove how different anchors' arrangement can lead to the same performance levels adopting far different numbers of anchors, thus obtaining target accuracy and keeping at the minimum the computational load.

The obtained results are shown in Figs. 13–15 for cases Decawave, BeSpoon, and Ubisense, respectively. In Figs. 13–15, there are two subplots: (a) and (b). In (a) to display the performance comparison between the two configurations, a colormap has been used. In detail, considering for both the configurations the mean localization error and its standard deviation, the different colors indicate the following.

1) *Green:* Configuration 2 is better than configuration 1.
2) *Yellow:* The two configurations are compatible with a 95% confidence level.
3) *Red:* Configuration 1 is better than configuration 2.

The number of anchors for configuration 2 and configuration 1 is shown on the x- and y-axes, respectively. In (b) instead, an error bar is shown considering the mean localization error and its expanded standard deviation ($k = 2$), for both the configurations by varying the number of anchors. Fig. 13–15 allows to extract the following information useful for designing an anchor-based UWB localization system, given the choices made for the simulation parameter values.

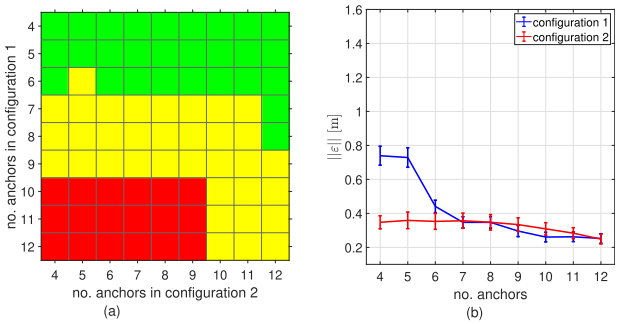

Fig. 14. Performance comparison between configurations 1 and 2. (a) Color map indicating the best configuration versus the number of anchors: green for configuration 2, red for configuration 1, and yellow in case of compatible results. (b) Norm of the localization error versus the number of anchors for both the configurations in the form of error (standard deviation) bar. BeSpoon case.

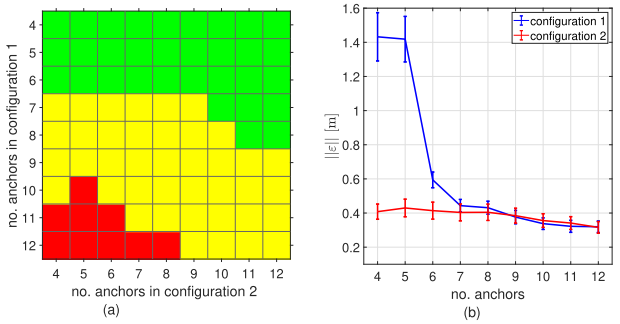

Fig. 15. Performance comparison between configurations 1 and 2. (a) Color map indicating the best configuration versus the number of anchors: green for configuration 2, red for configuration 1, and yellow in case of compatible results. (b) Norm of the localization error versus the number of anchors for both the configurations in the form of error (standard deviation) bar. Ubisense case.

1) With the same number of anchors, configuration 2 is winning for 4 and 5 anchors (Decawave) and for 4–6 anchors (BeSpoon and Ubisense) compared with configuration 1. As the number of anchors increases, compatible performance is always obtained. This means that the choice of which configuration to use is not important with a high number of anchors (>7), while with a low number of anchors (<7) configuration 2 offers better results.
2) Configuration 1 is strongly affected by the number of anchors. In fact, regardless of the devices, the monotonous trend is evident as the number of anchors increases. Consequently, adopting configuration 1, it is necessary to consider a high number of anchors (>7) to achieve good performance. For example, to have a mean localization error of about 30 cm, it is necessary to use seven anchors.
3) Configuration 2 is scarcely affected by the number of anchors. In fact, the obtained performance with four anchors is compatible up to a number of anchors equal to 10 (Decawave) and 11 (BeSpoon and Ubisense). Consequently, the adoption of configuration 2, enabling the homogeneous filling of all the planes with a constant number of anchors instead of filling one plane at a time, allows to get acceptable performance levels ($\epsilon = 30$ cm) with a low overall number of anchors and its increase does not impact the localization accuracy in depth.
4) When a different device is considered (with different metrological features), it is possible to provide two indications depending on which configuration is chosen. With configuration 1, the performance degradation associated with the metrological features worsening is present as the number of anchors varies. In particular, with Ubisense, performance is always worse than Decawave and BeSpoon, while the latter reaches performance compatibility from 6 anchors onward. With configuration 2, on the other hand, Decawave and BeSpoon always have compatible performance, but Ubisense is also compatible with the previous ones in scenarios having 4–9 anchors. In this case, the worsening of the metrological features is mitigated by a better spatial arrangement of the anchors.

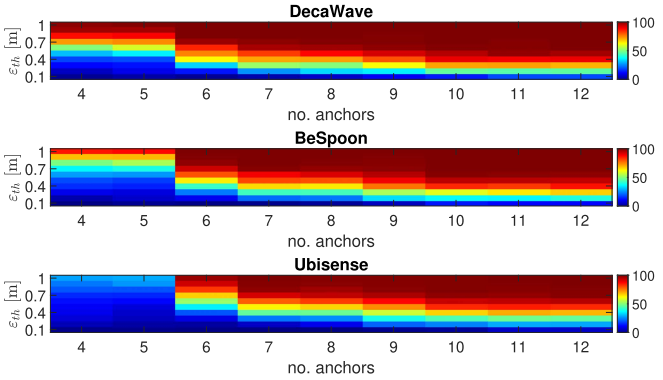

Fig. 16. Empirical cdfs of the localization error by varying the number of anchors and the error threshold for the considered devices, in configuration 1.

Subsequently, for each configuration and for each considered device, an empirical cdf was determined. Fig. 16 and 17 shows the obtained cdfs, where the number of anchors is shown on the x-axis, the error threshold (ε_{th}) is shown on the y-axis, and the colorbar represents the amplitude values of the cdf expressing the percentage of analyzed points with localization errors below the threshold. Fig. 16 and 17 shows the cdf for the considered devices for configuration 1 and configuration 2, respectively. These cdfs can be used to define the minimum number of anchors required to achieve target localization accuracies.

For example, Tables IV and V show a performance comparison for both the configurations, considering an error threshold of 60 cm. In detail, Tables IV and V show the percentage values of the empirical cdf ($\mathbf{F}$) and the lower (F_{low}) and upper (F_{up}) confidence limits for the values of the function $\mathbf{F}$. In particular, the values are represented with a confidence level equal to 95% (significance level $\alpha = 0.05$). It is noted that with a low number of anchors (<7), the obtained performance with configuration 1 is clearly worse than configuration 2. In fact, considering the Decawave kit, in configuration 1 percentages of about 84% are reached with six anchors, while in configuration 2 already with four anchors percentages of about 91% are reached. Similar considerations can be extracted for the BeSpoon and Ubisense kits. With a high number of anchors

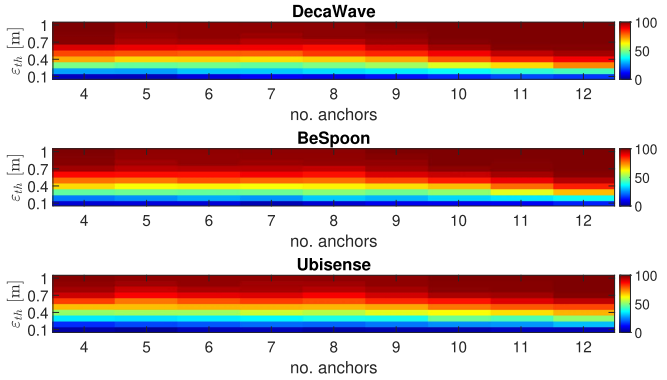

Fig. 17. Empirical cdfs of the localization error by varying the number of anchors and the error threshold for the considered devices, in configuration 1.

TABLE IV
COMPARISON OF DEVICE PERFORMANCE BY VARYING THE NO. ANCHORS, FOR CONFIGURATION 1 WHEN THE ERROR THRESHOLD IS 60 cm

No. anchors	**F** (F_{low}, F_{up}) **[%]** DecaWave	BeSpoon	Ubisense
4	**50.5** (43.8, 57.1)	**28.2** (22.2, 34.2)	**13.9** (9.3, 18.5)
5	**58.8** (52.2, 65.4)	**27.8** (21.8, 33.7)	**12.9** (8.5, 17.4)
6	**84.3** (79.4, 89.1)	**79.6** (74.2, 85.0)	**52.8** (46.1, 59.4)
7	**96.3** (93.8, 98.8)	**88.9** (84.7, 93.1)	**78.2** (72.7, 83.7)
8	**97.2** (95.0, 99.4)	**91.2** (87.4, 94.9)	**81.9** (76.8, 87.1)
9	**98.6** (97.0, 100.0)	**95.4** (92.6, 98.2)	**87.5** (83.1, 91.9)
10	**100.0** (100.0, 100.0)	**99.5** (98.6, 100.0)	**93.1** (89.7, 96.4)
11	**99.5** (98.6, 100.0)	**99.1** (97.8, 100.0)	**93.8** (90.8, 97.1)
12	**100.0** (100.0, 100.0)	**98.6** (97.5, 100.0)	**94.9** (91.9, 97.8)

TABLE V
COMPARISON OF DEVICE PERFORMANCES BY VARYING THE NO. ANCHORS, FOR CONFIGURATION 2 WHEN THE ERROR THRESHOLD IS 60 cm

No. anchors	**F** (F_{low}, F_{up}) **[%]** DecaWave	BeSpoon	Ubisense
4	**91.2** (87.4, 94.9)	**87.0** (82.6, 91.5)	**81.9** (76.8, 87.1)
5	**89.8** (85.8, 93.8)	**86.6** (82.0, 91.1)	**75.9** (70.2, 81.6)
6	**88.9** (84.7, 93.1)	**86.1** (81.5, 90.7)	**79.6** (74.2, 85.0)
7	**88.9** (84.7, 93.1)	**88.4** (84.1, 92.7)	**81.9** (76.8, 87.1)
8	**86.6** (82.0, 91.1)	**86.1** (81.5, 90.7)	**80.1** (74.7, 85.4)
9	**92.6** (89.1, 96.1)	**91.2** (87.4, 94.9)	**83.8** (78.8, 88.7)
10	**96.7** (94.4, 99.1)	**93.1** (89.7, 96.4)	**85.6** (80.9, 90.3)
11	**99.5** (98.6, 100.0)	**96.7** (94.4, 99.1)	**90.7** (86.8, 94.6)
12	**100.0** (100.0, 100.0)	**99.5** (98.6, 100.0)	**93.9** (90.8, 97.1)

(>7), both the configurations allow the achievement of the target performance with a percentage greater than 80% of cases. Finally, when the number of anchors is equal to 12, the two configurations show the same performance. This can be visualized through the intersection of the expressed confidence levels. These observations are consistent with those extracted from the previous results.

VI. CONCLUSION AND FUTURE DEVELOPMENTS

The localization of objects in indoor environments requires an accurate design phase. As novel contribution in this field, the authors have proposed and tested a widely applicable design tool in the framework of UWB technology. In particular, the research allows defining and implementing a simulation-to-experimental transfer tool for accurate prediction of localization performance levels whenever knowledge about the involved uncertainty models can be inferred and the device metrological features and domain characteristics are known. Indeed, by inputting target parameters and physical constraints, the design tool performs localization tests, and by adopting an uncertainty model of the environment and devices under test, it responses with the best combination of parameters ensuring target localization accuracy and minimum energy consumption. This is one of the main contributions of this article, in which a mathematical optimization model has been formalized, whose output provides setup optimal configurations to the implementers obtaining target performance under energy consumption constraints. It only needs domain dimensions and the knowledge of the uncertainty model of the ranging phase (the knowledge of the accuracy and repeatability levels of the distance measurements performed to get ranges tag–anchor). Consequently, positioning uncertainty derives from the uncertainty propagation law on the function mapping the raw ranging measurements to the 3-D coordinates of the tag position. It is worth to note that a methodology to compute the uncertainty model taking into account both device and environment contributions is a novel suitable contribution of this article allowing an improvement of simple adoption of device datasheets and avoiding to deal with complex radio-propagation models. Currently, such a model must be estimated *a priori*: in this version of the design tool, standard deviations adopted in the uncertainty model have been taken from a referenced paper. In our future research, we would like to develop a fast uncertainty model building by a very low number of measurements to be carried out in a first site inspection. The design simulation results have been validated with experimental tests, to prove the results' adherence to real trials on the field. As a general remark, we proved that the number of anchors is not the primary influence factor for performance levels, but their placement greatly changes the localization results. Such an outcome allows to get low-error localization results also in case of limited number of anchors, whenever devices' specifications are high level, or to decrease localization error by increasing the number of anchors, in case of low-end devices.

REFERENCES

[1] F. Jamil, N. Iqbal, S. Ahmad, and D.-H. Kim, "Toward accurate position estimation using learning to prediction algorithm in indoor navigation," *Sensors*, vol. 20, no. 16, p. 4410, Aug. 2020. [Online]. Available: https://www.mdpi.com/1424-8220/20/16/4410
[2] R. Zetik, G. Shen, and R. S. Thomä, "Evaluation of requirements for UWB localization systems in home-entertainment applications," in *Proc. Int. Conf. Indoor Positioning Indoor Navigat.*, Sep. 2010, pp. 1–8.
[3] J. Shang, S. Chen, J. Wu, and S. Yin, "ARSpy: Breaking location-based multi-player augmented reality application for user location tracking," *IEEE Trans. Mobile Comput.*, vol. 21, no. 2, pp. 433–447, Feb. 2022.
[4] M.-P. Lee, H.-Y. Hu, and N. Jafar, "Life chasing: A location-based game prototype for elderly health promotion," in *Proc. Int. Conf. Healthcare Service Manage. (ICHSM)*, New York, NY, USA, 2018, pp. 265–271, doi: 10.1145/3242789.3242834.
[5] G. P. Cimellaro, M. Domaneschi, and A. Z. Noori, "Improving post-earthquake emergency response using indoor tracking," *Earthq. Spectra*, vol. 36, no. 3, pp. 1208–1230, 2020, doi: 10.1177/8755293020911163.
[6] M. Zhou *et al.*, "Adaptive genetic algorithm-aided neural network with channel state information tensor decomposition for indoor localization," *IEEE Trans. Evol. Comput.*, vol. 25, no. 5, pp. 913–927, Oct. 2021.
[7] X. Liu *et al.*, "Kalman filter-based data fusion of Wi-Fi RTT and PDR for indoor localization," *IEEE Sensors J.*, vol. 21, no. 6, pp. 8479–8490, Mar. 2021.

[8] H. Rizk, A. Elmogy, and H. Yamaguchi, "A robust and accurate indoor localization using learning-based fusion of Wi-Fi RTT and RSSI," *Sensors*, vol. 22, no. 7, p. 2700, Mar. 2022. [Online]. Available: https://www.mdpi.com/1424-8220/22/7/2700
[9] J. Chen *et al.*, "A data-driven inertial navigation/Bluetooth fusion algorithm for indoor localization," *IEEE Sensors J.*, vol. 22, no. 6, pp. 5288–5301, Mar. 2022.
[10] M. Ridolfi, A. Kaya, R. Berkvens, M. Weyn, W. Joseph, and E. D. Poorter, "Self-calibration and collaborative localization for UWB positioning systems: A survey and future research directions," *ACM Comput. Surv. (CSUR)*, vol. 54, no. 4, pp. 1–27, 2021.
[11] A. Boukerche, H. A. B. Oliveira, E. F. Nakamura, and A. A. F. Loureiro, "Localization systems for wireless sensor networks," *IEEE Wireless Commun.*, vol. 14, no. 6, pp. 6–12, Dec. 2007.
[12] L. Ferrigno, G. Miele, F. Milano, V. Pingerna, G. Cerro, and M. Laracca, "A UWB-based localization system: Analysis of the effect of anchor positions and robustness enhancement in indoor environments," in *Proc. IEEE Int. Instrum. Meas. Technol. Conf. (I2MTC)*, May 2021, pp. 1–6.
[13] L. Ferrigno *et al.*, "Magnetic localization system for short-range positioning: A ready-to-use design tool," *IEEE Trans. Instrum. Meas.*, vol. 70, pp. 1–9, 2021.
[14] G. Cerro *et al.*, "On a finite domain magnetic localization by means of TMR triaxial sensors," in *Proc. IEEE Int. Instrum. Meas. Technol. Conf. (I2MTC)*, May 2020, pp. 1–6.
[15] *Trek1000 EVALUATION KIT User Manual*. Accessed: Jun. 4, 2022. [Online]. Available: https://www.decawave.com/wp-content/uploads/2018/09/trek1000_user_manual.pdf
[16] *BeSpoon—Inch-Level Tracking—Real-Time Location System*. Accessed: Jun. 4, 2022. [Online]. Available: https://bespoon.xyz/
[17] *Ubisense Series 7000 IP Sensors*. Accessed: Jun. 4, 2022. [Online]. Available: https://www.yumpu.com/en/document/read/34089792/ubisense-series-7000-ip-sensors
[18] T. Gigl, P. Meissner, J. Preishuber-Pfluegl, and K. Witrisal, "Ultra-wideband system-level simulator for positioning and tracking (U-SPOT)," in *Proc. Int. Conf. Indoor Positioning Indoor Navigat.*, Sep. 2010, pp. 1–9.
[19] N. Amiot, M. Laaraiedh, and B. Uguen, "PyLayers: An open source dynamic simulator for indoor propagation and localization," in *Proc. IEEE Int. Conf. Commun. Workshops (ICC)*, Jun. 2013, pp. 84–88.
[20] T. Jankowski and M. Nikodem, "SMILe–simulator for methods of indoor localization," in *Proc. Int. Conf. Indoor Positioning Indoor Navigat. (IPIN)*, Sep. 2018, pp. 206–212.
[21] M. C. Pérez-Rubio *et al.*, "Simulation tool and online demonstrator for CDMA-based ultrasonic indoor localization systems," *Sensors*, vol. 22, no. 3, p. 1038, Jan. 2022.
[22] F. Zafari, A. Gkelias, and K. K. Leung, "A survey of indoor localization systems and technologies," *IEEE Commun. Surveys Tuts.*, vol. 21, no. 3, pp. 2568–2599, 3rd Quart., 2017.
[23] A. R. J. Ruiz and F. S. Granja, "Comparing ubisense, bespoon, and decawave UWB location systems: Indoor performance analysis," *IEEE Trans. Instrum. Meas.*, vol. 66, no. 8, pp. 2106–2117, Aug. 2017.
[24] J. Vishwesh and P. Raviraj, "Ultra wideband (UWB): Characteristics and applications," *Int. J. Recent Trends Eng. Res.*, vol. 4, no. 6, pp. 45–52, Jun. 2018.
[25] *IEEE Standard for Low-Rate Wireless Networks*, IEEE Standard 802.15.4-2015 (Revision of IEEE Standard 802.15.4-2011), Apr. 2016, pp. 1–709.

Gianni Cerro (Member, IEEE) is currently a Research Fellow with the Department of Medicine and Health Sciences, University of Molise, Campobasso, Italy. His research interests include magnetic localization systems for biomedical and industrial applications, cognitive radio systems for new-generation communication technologies, measurements in telecommunication networks, sensor networks for environmental monitoring, and measurement characterization of medical devices, such as brain–computer interfaces.

Luigi Ferrigno (Senior Member, IEEE) has been a Full Professor of electric and electronic measurement and the Scientific Manager of the Industrial Measurements Laboratory, University of Cassino and Southern Lazio, Cassino, Italy, since 2004. In 2008, he was a Founding Member of the university spin-off, Spring Off (University of Salerno), Fisciano, Italy. He is an NDE4.0 Ambassador for the Italian Association of Non-Destructive Evaluation and Test (AiPnD) in the EFNDT WG10. He coordinated and participated in several national and international research projects. His current research interests include the NDT4.0, novel learning sensors and measurement systems for smart city, the Internet of Things (IoT), automotive, smart energy, and environment.

Marco Laracca (Member, IEEE) received the M.S. degree in electrical engineering and the Ph.D. degree in electrical and information engineering from the University of Cassino and Southern Lazio, Cassino, Italy, in 2002 and 2006, respectively.

From 2006 to 2021, he was an Assistant Professor of electrical and electronic measurements with the University of Cassino and Southern Lazio. Since 2021, he has been an Associate Professor of electrical and electronic measurements with the Sapienza University of Rome, Rome, Italy. He has also been the Chief of the ACCREDIA Notified Metrology Laboratory (LAT 105), University of Cassino and Southern Lazio, since 2018. His current research interests include realization of measurement system for nondestructive testing, sensor realization and characterization, electric measurement under nonsinusoidal conditions, and speed calibration.

Gianfranco Miele (Senior Member, IEEE) is currently an Associate Professor with the Department of Electrical and Information Engineering, University of Cassino and Southern Lazio, Cassino, Italy. His current research interests include design and implementation of innovative methods for performance assessment of RF telecommunication systems and communication networks.

Filippo Milano (Student Member, IEEE) received the M.S. degree *(cum laude)* in electrical engineering and the Ph.D. degree in methods, models, and technologies per engineering from the University of Cassino and Southern Lazio, Cassino, Italy, in 2018 and 2021, respectively.

He is currently a Research Fellow with the Department of Electrical and Information Engineering, University of Cassino and Southern Lazio. His research interests include design, implementation, and characterization of positioning systems for biomedical and industrial applications, development of models and techniques for predictive batteries' diagnosis, and thicknesses' estimation of metal laminates using eddy current techniques.

Valentina Pingerna received the M.S. degree *(cum laude)* in computer science engineering from the University of Cassino and Southern Lazio, Cassino, Italy, in 2020.

She has been a Research Assistant with the University of Cassino and Southern Lazio. Her research interests include measurement characterization of biometric systems and implementation of algorithms for indoor localization.